Multiuser Interference and Inter-Frame Interference in UWB Transmitted Reference Systems

Klaus Witrisal
Graz University of Technology
Inffeldgasse 12, A-8010 Graz, Austria
email: Witrisal@inw.tugraz.at

Marco Pausini and Antonio Trindade
Delft University of Technology
Mekelweg 4, NL-2628 CD Delft, The Netherlands
email: {M.Pausini,A.Trindade}@ewi.tudelft.nl

***Abstract*—In transmitted reference ultra-wideband (TR-UWB) systems and differential transmitted reference (DTR-UWB) systems, the performance is, besides to noise, determined by interference among pulses due to the dispersive multipath radio channel (inter-frame interference). The multiple access interference is also heavily influenced by multipath propagation. As a first step towards the analysis and optimization of such systems, this paper analyzes statistically the response of the pulse-pair correlators including integrate and dump circuitry, which are the basic building block of TR-UWB receivers, to desired and un-desired pulse-pairs. Results are given in terms of basic channel parameters like RMS delay spread and Ricean K-factor. As an example for the application of our analysis, we present a novel multiuser DTR-UWB system.**

I. Introduction

In transmitted reference UWB receivers [1]–[4], the received signal consisting of a train of pulses is correlated with itself, using a (set of) "pulse-pair" correlators at fixed correlation lag(s). If a pulse-pair spaced by a given lag is present, a high correlation output is obtained, which is used to detect the data. Data can be applied, for instance, by changing the polarity of one of the pulses. Generally, the first pulse is denoted as the "reference pulse" and the second pulse is the "data pulse". The reference pulse acts as a template signal for the (auto-) correlation receiver.

Due to multipath propagation, other pulses in the transmitted signal also lead to correlator outputs and thus to a distortion of the desired signal, termed inter-frame interference (IFI). The main goal of this study is the statistical characterization of the correlator output as a function of simple channel parameters for the case of (heavy) IFI, which is novel work to the authors' knowledge. Many previous studies consider limited or no IFI (e.g. [2]), do not specify the IFI (e.g. [3]), or derive the IFI from data of individual channel realizations (e.g. [4]).

The paper also presents a novel multiuser (MU) differential TR-UWB system including a basic receiver scheme providing multiuser separation. The effect of (heavy) multipath interference is derived, applying the analytical results obtained.

This paper is organized as follows. Basic signal and channel models are introduced in Section II. In Section III, the novel MU-DTR-UWB system is shown. The analysis of IFI is presented in Section IV, followed by the (simplified) study of the MU-DTR system in Section V. Computer simulation and analytical results are given in Section VI. Conclusions are drawn in Section VII.

II. Signal and Channel Model

An impulse radio UWB-system sends data as a stream of very narrow pulses. Including the transmitter and receiver antennas and circuitry, we denote the received (template) pulse-shape as $w(t)$, in absence of a multipath radio channel. This pulse is confined in time to an interval $t \in [0, T_w)$, i.e., $w(t) = 0$ for $t < 0$ or $t \geq T_w$. A standard pulse-shape assumed in theoretical work is the second derivative of a Gaussian pulse, $w(t) = [1 - 4\pi(t/\tau_m)^2] \exp[-2\pi(t/\tau_m)^2]$, specified by the parameter τ_m.

The channel response is modeled as a sum of delta-pulses,

$$h(t) = \sum_{i=0}^{\infty} \alpha_i \delta(t - \tau_i), \qquad (1)$$

where α_i are independent zero-mean random variables, except for α_0, which is non-zero mean accounting for a dominant line-of-sight (LOS) path. τ_i are discrete ray-arrival times, where $\tau_0 = 0$ is assumed to be the first multipath component arriving. Note that the number of arriving rays is not specified but the ray amplitudes become negligibly small for large τ_i. Moreover, the channel is assumed to be time-invariant.

The channel is characterized by its delay power spectrum (or average power delay profile), $P_h(t) = \mathrm{E}\{h^2(t)\} = E\left\{\sum_{i=0}^{\infty} \alpha_i^2 \delta(t - \tau_i)\right\}$.

The expected power of a ray at delay τ_i is given by

$$E\{\alpha_i^2 | \tau_i\} = \begin{cases} \rho^2 & i = 0 \\ \frac{P_h(\tau_i)}{\lambda(\tau_i)} & i > 0 \end{cases}, \qquad (2)$$

where $\lambda(t)$ [rays/s] is the density of arriving rays, being a function of the excess delay time t.

A. Channel Description

In this work, the delay power spectrum $P_h(t)$ (in [W/s]) is described by an exponentially decaying part and a pulse at excess delay time $t = 0$ to account for the direct-path in LOS channels.

$$P_h(t) = \rho^2 \delta(t) + \widetilde{P}_h(t) = \begin{cases} 0 & t < 0 \\ \rho^2 \delta(t) & t = 0 \\ \Pi e^{-\gamma t} & t > 0 \end{cases} \qquad (3)$$

As derived in [5], the parameters in (3) can be expressed in terms of the channel parameters P_0: the (normalized) received power, K: the Ricean K-factor defining the power ratio of the LOS-path to the scattered paths, and τ_{rms}: the RMS delay spread of the channel. These relations are

$$\rho^2 = P_0 \frac{K}{K+1} \qquad (4)$$

$$\gamma = \frac{1}{\tau_{rms}} \frac{\sqrt{2K+1}}{K+1} \qquad (5)$$

$$\Pi = \frac{P_0}{K+1} \gamma. \qquad (6)$$

This work was partially funded by the Dutch Min. Econ. Affairs/Min. Education Freeband-impulse project *Airlink*.

0-7803-8373-7/04/$20.00 ©2004 IEEE

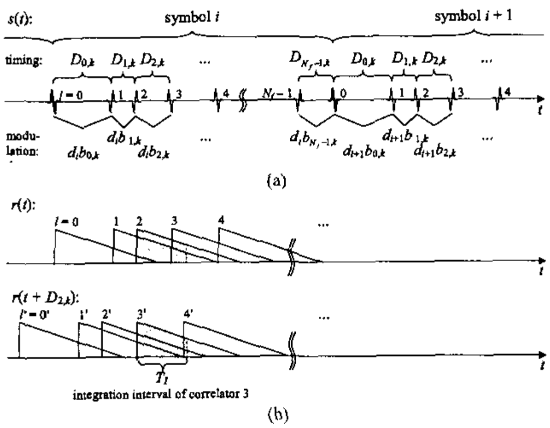

Fig. 1. Diagram of the transmitted and received signals in the proposed UWB-DTR system for multiuser detection.

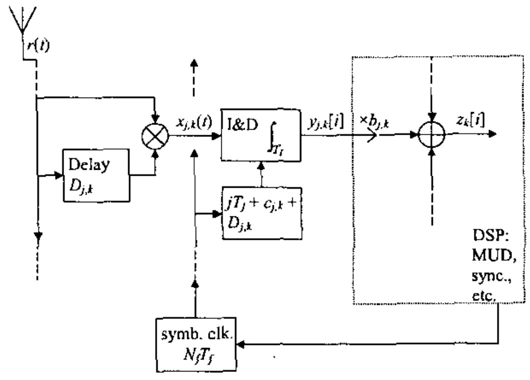

Fig. 2. Pulse pair correlator used in the multiuser differential transmitted reference UWB receiver.

III. Multiuser Differential TR System

In this section, a novel multiuser differential TR-UWB system is presented. We will use this system as an example for demonstrating the analysis of intersymbol and multiuser interference due to multipath propagation.

Each data symbol $d_i \in \{-1,+1\}$, i being the symbol index, is transmitted via N_f consecutive pulses/frames. A known random sequence $b_{j,k} \in \{-1,+1\}$ is differentially modulated on the time-hopped pulses, where $j \in \{0,1,...,N_f-1\}$ is the pulse index within a symbol and k is the user index. Superimposing the user data and the frame-level code, the differentially modulated pulse-polarities are obtained as $a_{i,j+1,k} = a_{i,j,k}b_{j,k}d_i$ and $a_{i+1,0,k} = a_{i,N_f-1,k}b_{N_f-1,k}d_i$. The transmitted signal is written

$$s_k(t) = \sum_{i=-\infty}^{\infty}\sum_{j=0}^{N_f-1} a_{i,j,k}\widetilde{w}(t-t_{i,j,k}), \tag{7}$$

using $\widetilde{w}(t)$ as the transmitted pulse shape.

The time-instants of the pulses are defined as $t_{i,j,k} = (j + iN_f)T_f + c_{j,k}$, where T_f is the average frame duration (average spacing between two pulses) and $c_{j,k}$ is the known time-hopping (TH) sequence. Important for the proposed scheme are the time shifts between consecutive pulses, written as $D_{j,k} = t_{i,j+1,k} - t_{i,j,k}$. The transmitted signal is visualized in Fig. 1(a).

A bank of pulse-pair correlators, whose lags are matched to the time-shifts $D_{j,k}$, is present at the input of a receiver for such signals, as shown in Fig. 2. The integrate-and-dump (I&D) blocks are triggered at the arrival-times of the respective pulses, which requires time-synchronization and knowledge of the TH-sequence. Integration is performed over a time interval T_I. The outputs of these blocks may be sampled at the symbol rate. The basic receiver shown here coherently combines these outputs by removing the chip-level modulation $b_{j,k}$. We obtain

$$z_k[i] = \sum_{j=0}^{N_f-1} y_{j,k}[i]b_{j,k} \tag{8}$$

$$y_{j,k}[i] = \int_{t_{i,j,k}}^{t_{i,j,k}+T_I} r(t+D_{j,k})r(t)\,dt, \tag{9}$$

where $r(t) = s_k(t) * h(t) * f_{rx}(t)$ for the desired signal and without channel noise. $f_{rx}(t)$ denotes a front-end analog filter in the receiver that is not shown in Fig. 2.

In this paper we do not consider noise. In stead, we study the impact of the time-dispersive multipath channel, which leads to interference among pulses (termed inter-frame interference) if the maximum excess delay of the channel is lager than $\min\{D_{j,k} : j \in [0,N_f)\}$, as visualized in Fig. 1(b). Our goal is the stochastic description of the channel's impact on the output of the integrate-and-dump blocks.

A. Impact of the Multipath Channel

We analyze the output of a single correlator (9)

$$y_{j,k}[i] = \int_{t_{i,j,k}}^{t_{i,j,k}+T_I} \sum_{i,l} a_{i,l,k}g(t-t_{i,l,k}) \times \sum_{i',l'} a_{i',l',k}g(t-t_{i',l',k}+D_{j,k})\,dt, \tag{10}$$

where $g(t) = h(t) * w(t) = \sum_{i=0}^{\infty}\alpha_i w(t-\tau_i)$ is the received signal in response to a single radiated UWB-pulse. $w(t) = \widetilde{w}(t) * f_{rx}(t)$ is the received prototype pulse shape.

To study this equation, we define

$$I(t_1,t_2;\tau) = \int_{t_1}^{t_2} g(\mu)g(\mu+\tau)\,d\mu, \tag{11}$$

where τ is the correlation lag and t_1, t_2 are the integration borders that are given by clearing and sampling the integrators. The expectation and variance of $y_{j,k}[i]$ are two basic measures for the influence of IFI on the receiver. These parameters will be derived in Section V, which will require the statistical analysis of the integral (11), being the main topic of this paper.

IV. Stochastic Analysis of $I(t_1,t_2;\tau)$

For an ensemble of channel realizations, the integral $I(t_1,t_2;\tau)$ (11) can be seen as a random variable. In this section, the statistical moments of this random variable are derived up to second order. We assume that $\tau > 0$. Due to symmetry, $I(t_1,t_2;\tau) = I(t_1+\tau,t_2+\tau;-\tau)$ for $\tau < 0$.

A. Expected Value of $I(t_1, t_2; \tau)$

Calculating the expectation of $I(t_1, t_2; \tau)$ requires the analysis of the expectation of the product $g(t)g(t+\kappa)$,

$$E\{I(t_1,t_2;\tau)\} = \int_{t_1}^{t_2} E\{g(\mu)g(\mu+\tau)\}\, d\mu$$

$$E\{g(t)g(t+\kappa)\} = E\left\{\sum_{i=0}^{\infty}\alpha_i w(t-\tau_i)\sum_{j=0}^{\infty}\alpha_j w(t+\kappa-\tau_j)\right\} = \sum_{i=0}^{\infty}\sum_{j=0}^{\infty} E\{\alpha_i w(t-\tau_i)\alpha_j w(t+\kappa-\tau_j)\}.$$

Since the random variables $\{\alpha_i\}$ are uncorrelated (envoking the uncorrelated scattering property of the channel), $E\{\alpha_i\alpha_j\} = 0$ for $i \neq j$, and the expression can be written

$$\begin{aligned} E\{g(t)g(t+\kappa)\} &= \sum_{i=0}^{\infty} E\{\alpha_i^2 w(t-\tau_i)w(t+\kappa-\tau_i)\} \\ &= [w(t)w(t+\kappa)] * E\left\{\sum_{i=0}^{\infty}\alpha_i^2\delta(t-\tau_i)\right\} \\ &= [w(t)w(t+\kappa)] * P_h(t) \qquad (12) \\ &= \int_0^{T_w} w(\mu)w(\mu+\kappa)P_h(t-\mu)\, d\mu \\ &\approx \rho^2 w(t)w(t+\kappa) + \widetilde{P}_h(t)\phi_w(\kappa), \qquad (13) \end{aligned}$$

where $\phi_w(\kappa) = \int_0^{T_w} w(\mu)w(\mu+\kappa)\, d\mu$ is the autocorrelation of the received (prototype) pulse $w(t)$. We define $\phi_w(0) = 1$, i.e., the prototype pulse is assumed to have unit energy.

The approximation in (13) assumes that $\widetilde{P}_h(\mu)$ is approximately constant over the integration range of the convolution integral, $\mu \in [t - T_w, t]$. This assumption is reasonable since usually $T_w \ll 1/\gamma$. (Recall that γ is the decay exponent of the decaying part of the delay power spectrum $\widetilde{P}_h(t)$.) However, some (negligible) error is made if $t \in [0, T_w)$, since $\widetilde{P}_h(\mu) = 0$ for $\mu < 0$.

It is evident that, according to the model used, the channel is uncorrelated for lags greater than the support of $\phi_w(\kappa)$. Received pulse shapes varying with the excess delay of the channel impulse response can be incorporated in (12) by introducing $w(t,\kappa)$, which depends on the excess delay variable t.

With (13) and (3), we finally obtain the expectation of $I(t_1, t_2; \tau)$, assuming that $t_2 > 0$ and $t_2 > t_1$

$$E\{I(t_1,t_2;\tau)\} \approx P_0\phi_w(\tau)\begin{cases} \left[1 - \frac{1}{K+1}e^{-\gamma t_2}\right] & t_1 \leq 0 \\ \frac{1}{K+1}\left[e^{-\gamma t_1} - e^{-\gamma t_2}\right] & t_1 > 0 \end{cases}. \qquad (14)$$

The parameter γ is given in (6).

This equation shows that, on the average, there is no IFI if the correlation lag is greater than the support of $\phi_w(\tau)$, $|\tau| > T_w$. For a single channel realization, this may not be the case however, since $I(t_1, t_2; \tau)$ is a random variable. In the next section, we evaluate the second moment of this expression.

B. Variance of $I(t_1, t_2; \tau)$ for $|\tau| > T_w$

For $|\tau| > T_w$, the second moment of $I(t_1, t_2; \tau)$ equals the variance, since $I(t_1, t_2; \tau)$ then is a zero-mean random processes. It is derived from

$$E\{I^2(a,b;\tau)\} = \int_a^b \int_a^b E\{g(\mu)g(\mu+\tau)\, g(\nu)g(\nu+\tau)\}\, d\mu d\nu. \qquad (15)$$

Considering that $g(t)$ and $g(t+\tau)$ are uncorrelated for $|\tau| > T_w$ and $g(t)$ is zero mean for $t > T_w$, we can split up the expectation term in two terms of the form of (12). This yields

$$\begin{aligned} E\{I^2(a,b;\tau)\} &= \qquad (16) \\ &= \int_a^b \int_a^b E\{g(\mu)g(\nu)\}\, E\{g(\mu+\tau)g(\nu+\tau)\}\, d\mu\, d\nu \\ &\approx \int_a^b \int_{-\infty}^{\infty} E\{g(\mu)g(\mu+\kappa)\}\, E\{g(\mu+\tau)g(\mu+\kappa+\tau)\}\, d\kappa\, d\mu \end{aligned}$$

where $\nu = \mu + \kappa$ has been used. The second equation is an approximation due to the integration interval $\kappa \in (-\infty, \infty)$ used for simplicity, in stead of $\kappa \in [a - \mu, b - \mu]$.

We continue our derivation using (13). Carefully considering the LOS ray at $t = 0$, it can be shown that the second moment can be approximated as

$$E\{I^2(a,b;\tau)\} \approx \int_{-T_w}^{T_w} \phi_w^2(\kappa)\, d\kappa \int_a^b P_h(\mu)P_h(\mu+\tau)\, d\mu. \qquad (17)$$

Again we have assumed that $\widetilde{P}_h(\mu + \tau)$ is constant within the integration range $\mu \in [0, T_w)$, since $T_w \ll 1/\gamma$. Evaluating the second integral in this result with (3) yields

$$E\{I^2(t_1,t_2;\tau)\} = \frac{\gamma P_0^2}{(K+1)^2}\int_{-T_w}^{T_w} \phi_w^2(\kappa)\, d\kappa\, e^{-\gamma\tau} \times \begin{cases} \left[K + \frac{1}{2}\left(1 - e^{-2\gamma t_2}\right)\right] & t_1 \leq 0 \\ \frac{1}{2}\left(e^{-2\gamma t_1} - e^{-2\gamma t_2}\right) & t_1 > T_w \end{cases}. \qquad (18)$$

γ is given by (6) in terms of channel parameters. It is most remarkable that this result (for $\tau > T_w$) is independent of the distribution function of the channel taps and of the ray arrival process. The delay power spectrum $P_h(t)$, described in this paper by a simple model, determines this important parameter.

C. Variance of $I(t_1, t_2; \tau)$ for $\tau = 0$

The variance of $I(t_1, t_2; 0)$ is calculated as

$$\begin{aligned} \mathrm{var}\{I(a,b;0)\} &= E\{I^2(a,b;0)\} - E^2\{I(a,b;0)\} \\ &= \int_a^b \int_a^b E\{g^2(\mu)g^2(\nu)\}\, d\nu d\mu - \left[\int_a^b E\{g^2(\mu)\}\, d\mu\right]^2 \\ &\approx \int_a^b \int_{-T_w}^{T_w} E\{g^2(\mu)g^2(\mu+\kappa)\}\, d\kappa d\mu \\ &\quad - \int_a^b \int_{-T_w}^{T_w} E\{g^2(\mu)\}E\{g^2(\mu+\kappa)\}\, d\kappa d\mu. \end{aligned}$$

The change of the integration variable $\nu = \mu + \kappa$ and the approximation are equivalent to the derivation in (16). The integration range of κ can be confined to $\kappa \in (-T_w, T_w)$ since $E\{g^2(\mu)g^2(\mu+\kappa)\} = E\{g^2(\mu)\}E\{g^2(\mu+\kappa)\}$ if $|\kappa| > T_w$.

After some computations, which are omitted in this paper due to size restrictions, we obtain

$$\begin{aligned} &\mathrm{E}\{g^2(t)g^2(t+\kappa)\} - \mathrm{E}\{g^2(t)\}\mathrm{E}\{g^2(t+\kappa)\} \approx \\ &\approx \widetilde{R}_h(t)\phi_{w^2}(\kappa) + 2\widetilde{P}_h^2(t)\phi_w^2(\kappa) \\ &\quad + 4\rho^2\widetilde{P}_h(0)w(t)w(t+\kappa)\int_0^t w(\mu)w(\mu+\kappa)\, d\mu, \qquad (19) \end{aligned}$$

where $\phi_{w^2}(\kappa) = \int_{-\infty}^{\infty} w^2(t)w^2(t+\kappa)\,dt$ and $\widetilde{R}_h(t) = E\{\alpha_i^4|\tau_i = t\}\lambda(t)$ is related to the forth moment of the ray amplitudes. For Nakagami distributed rays characterized by m,

$$E\{\alpha_i^4|\tau_i = t\} = \left[\frac{\widetilde{P}_h(t)}{\lambda(t)}\right]^2 \left(1+\frac{1}{m}\right).$$

The variance is calculated from (19) by integrating over t and κ. Introducing the channel model (3) and assuming that the ray-density $\lambda(t) = \lambda$ is constant and that all rays are Nakagami distributed with a constant parameter m, we get the following expression for the variance of $I(t_1, t_2; \tau)$ at $\tau = 0$,

$$\begin{aligned}\mathrm{var}\{I(t_1,t_2;0)\} &\approx \frac{P_0^2\gamma}{(K+1)^2} \times \\ &\times \left(\left[\frac{1}{2\lambda}\left(1+\frac{1}{m}\right)\int_{-T_w}^{T_w}\phi_{w^2}(\kappa)\,d\kappa + \int_{-T_w}^{T_w}\phi_w^2(\kappa)\,d\kappa\right]\right. \\ &\times \begin{cases}\left[e^{-2\gamma t_1} - e^{-2\gamma t_2}\right] & t_1 > 0\\ \left[1 - e^{-2\gamma t_2}\right] & t_1 \le 0\end{cases} \\ &\left. + \begin{cases}0 & t_1 > 0\\ 2K\int_{-T_w}^{T_w}\phi_w^2(\kappa)\,d\kappa & t_1 \le 0\end{cases}\right), \end{aligned} \tag{20}$$

where γ is defined in (6). If $K = 0$, this result simplifies.

D. Covariance $\mathrm{cov}\{I(t_1,t_2;\tau_1)I(t_3,t_4;\tau_2)\}$

Writing the expectation $\mathrm{E}\{I(t_1,t_2;\tau_1)I(t_3,t_4;\tau_2)\}$ equivalently to (15), it can be shown that the covariance is zero, except if $|\tau_1 - \tau_2| < T_w$. That is, two integrator outputs are uncorrelated if their integration lags are sufficiently different. If $\tau_1 = \tau_2 = \tau$, the covariance becomes

$$\begin{aligned}&\mathrm{cov}\{I(t_1,t_2;\tau)I(t_3,t_4;\tau)\} = \\ &\quad = \mathrm{var}\{I(\max(t_1,t_3),\min(t_2,t_4);\tau)\}.\end{aligned} \tag{21}$$

The covariance is also zero, if $\max(t_1,t_3) > \min(t_2,t_4)$, i.e., $t_2 < t_3$ (assuming $t_1 < t_2$ and $t_3 < t_4$), which means that the integration intervals are non-overlapping.

E. Distribution Function

Since the integral expression (11) is essentially a sum of a large number of independent random variables (the products $g(t)g(t+\tau)$ consisting of large numbers of channel rays), we assume the correlator output to be described by a Gaussian random variable with a mean value given by (14) and a variance given by (18) or (20). Computer simulation results confirm this assumption for relatively rich scattering environments (high ray density λ).

V. Stochastic Analysis of the MU-DTR System

Purpose of this section is the derivation of the mean and variance of the pulse-pair correlator outputs, $y_{j,k}[i]$. Using (11) and substituting $l = j+m$ and $l' = j+n+1$, (10) can be written as

$$\begin{aligned}y_{j,k}[i] = &\sum_{m=-A}^{B}\sum_{n=-A}^{B} a_{i,j+m,k}a_{i,j+n+1,k} \\ &\times I(t_{i,j,k} - t_{i,j+m,k}, t_{i,j,k} - t_{i,j+m,k} + T_I; \\ &\quad D_{j,k} + t_{i,j+m,k} - t_{i,j+n+1,k}).\end{aligned} \tag{22}$$

The summation indices $m, n \in [-A, B]$ account for all pulses that contribute to the correlator output due to multipath. In the received signal illustrated in Fig. 1(b), the pulses $l = \{0,1,2,3\}$ and $l' = \{1',2',3',4'\}$ have impact within the integration interval shown. Generally, A is related to the maximum excess delay of the channel impulse response τ_{max}, $A = \lceil \tau_{max}/T_f \rceil$ and B to the integration interval $B = \lceil T_I/T_f \rceil$. For simplicity, we assume in this work that all interfering pulses belong to the same symbol with index i, i.e., inter-symbol interference is neglected.

A. Expectation of $y_{j,k}[i]$

Furthermore, we assume that a time-hopping code has been used, which ensures that all time-intervals are different. To be specific, $|D_{j,k} - D_{j',k}| > T_w$ for $j \neq j'$. Under this assumption, the expectations of the $I(a,b;\tau)$-terms in (22) will be zero except for $m = n = 0$ (see Section IV-A). Thus

$$\begin{aligned}E\{y_{j,k}[i]\} &= a_{i,j,k}a_{i,j+1,k}E\{I(0,T_I;0)\} \\ &= b_{j,k}d_iE\{I(0,T_I;0)\},\end{aligned} \tag{23}$$

which can be evaluated using (14).

B. Variance of $y_{j,k}[i]$

For the evaluation of the variance of $y_{j,k}[i]$, we assume that all $I(a,b;\tau)$-terms in (22) are uncorrelated, since either the lags τ or the integration ranges $t \in [a,b]$ are different (see Section IV-D). Under this assumption, the variances of the $I(a,b;\tau)$-terms can be simply summed up. Furthermore, we approximate the delays and arrival times by their mean values $(t_{i,j,k} - t_{i,j+m,k}) \approx -mT_f$ and $(D_{j,k} + t_{i,j+m,k} - t_{i,j+n+1,k}) \approx (m-n)T_f$, yielding

$$\begin{aligned}\mathrm{var}\{y_{j,k}[i]\} \approx &\sum_{m=-A}^{B}\sum_{n=-A}^{B} a_{i,j+m,k}^2 a_{i,j+n+1,k}^2 \\ &\times \mathrm{var}\{I(-mT_f, -mT_f + T_I; (m-n)T_f)\}.\end{aligned} \tag{24}$$

Selecting $T_I = T_f$, this result can be simplified to

$$\begin{aligned}\mathrm{var}\{y_{j,k}[i]\} \approx\, &2\sum_{l=1}^{A}\mathrm{var}\{I(0,\infty;lT_f)\} \\ &+ \mathrm{var}\{I(T_f,\infty;\tau\approx 0)\} + \mathrm{var}\{I(0,T_f;0)\},\end{aligned} \tag{25}$$

where $\mathrm{var}\{I(T_f,\infty;\tau\approx 0)\}$ denotes the variance for $|\tau| > T_w$ as derived in Section IV-B, however, evaluated at $\tau = 0$. For $K = 0$, using (18) and (20), the following expression is obtained.

$$\begin{aligned}&\mathrm{var}\{y_{j,k}[i]\} \approx \\ &\approx \frac{P_0^2}{2\tau_{rms}}\left\{\int_{-T_w}^{T_w}\phi_w^2(\kappa)\,d\kappa\left[\frac{2}{1-e^{-T_f/\tau_{rms}}} - e^{-\frac{2T_f}{\tau_{rms}}}\right]\right. \\ &\quad \left. + \frac{1}{2\lambda}\left(1+\frac{1}{m}\right)\int_{-T_w}^{T_w}\phi_{w^2}(\kappa)\,d\kappa\right\}\end{aligned} \tag{26}$$

In a very similar fashion, the variance of $y_{j,k'}[i]$ can be derived, when the receiver uses a different time-hopping code k' than the transmitter. For this derivation we have additionally assumed that the time-hopping codes are 'orthogonal', that is, for all interfering pulses $|D_{j,k} - D_{j',k'}| > T_w$. The simplified end result holds again for $K = 0$.

$$\begin{aligned}\mathrm{var}\{y_{j,k'}[i]\} &\approx 2\sum_{l=1}^{A}\mathrm{var}\{I(0,\infty;lT_f)\} + \mathrm{var}\{I(0,\infty;\tau\approx 0)\} \\ &\approx \frac{P_0^2}{2\tau_{rms}}\int_{-T_w}^{T_w}\phi_w^2(\kappa)\,d\kappa\,\coth\left(\frac{T_f}{2\tau_{rms}}\right)\end{aligned} \tag{27}$$

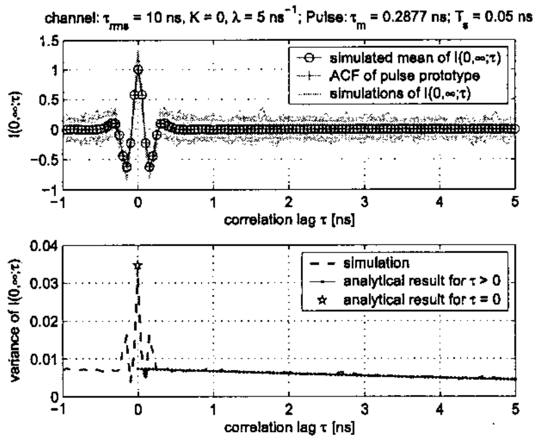

Fig. 3. Upper plot: simulation of $I(0,\infty;\tau)$ (light lines) and the average of 1000 simulations (line indicated by '∘'). Lower plot: variance of $I(0,\infty;\tau)$. Analytical results and computer simulations.

The analytical derivation of the variance of $z_k[i]$ requires the analysis of the cross-correlation of the outputs of multiple correlators $y_{j,k}[i]$. This is subject for future work. In the next section, our analytical results are compared to computer simulations.

VI. Simulation Results and Discussion

A. Channel Simulation Procedure

The channel simulator first generates an unquantized vector of ray arrival times according to a Poisson process with a constant mean ray arrival rate of $\lambda = 5$ ns^{-1} and a vector of Rayleigh distributed ray magnitudes with random polarity. In the mean for many channel simulations, the normalized received power $P_0 = 1$, the RMS delay spread $\tau_{rms} = 10$ ns, and the K-parameter $K = 0$, i.e., a non-LOS channel has been simulated.

The second derivative of a Gaussian pulse is used as a template pulse, $w(t+.35) = [1 - 4\pi(t/\tau_m)^2]\exp[-2\pi(t/\tau_m)^2]$ with $\tau_m = 0.2877$ ns and $t \in [0, 0.7]$ ns. This pulse is sampled in accordance to the sampling theorem, using the sampling period $T_s = 0.05$ ns. The precise position of the pulses in each channel impulse response has been oversampled, however, in order to represent better the unquantized ray arrival times. That is, in our simulations, the pulse position resolution has been choosen $T_{res} = 0.005$ ns.

B. Fundamental Integrator Output

The upper plot of Fig. 3 shows samples of the simulated correlation function $I(0,\infty;\tau)$ (for $t_1 = 0$ and $t_2 = \infty$) and the average of 1000 simulations. At very small correlation lags, the autocorrelation function $\phi_w(\tau)$ of the template pulse can be seen. For larger correlation lags, the mean of $I(0,\infty;\tau)$ is zero, as predicted by the analysis. The 'light' lines indicate the simulation results for a single channel realization each. It is evident, that these results deviate from the mean.

The variance of this deviation is analyzed in the lower plot of Fig. 3. Simulation results are compared with the analytical results obtained from (18) and (20). The agreement of the two traces is good, except for correlation lags $\tau \in (0, T_w)$, for which the analysis is not appropriate.

TABLE I
STATISTICS OF THE CORRELATOR OUTPUT

$k = k'$	τ_{rms} [ns]	analytical $y_{j,k}[i]$ mean	analytical $y_{j,k}[i]$ stdv	simulation $y_{j,k}[i]$ mean	simulation $y_{j,k}[i]$ stdv	simulation $z_k[i]$ mean	simulation $z_k[i]$ stdv
yes	2	0.99	0.42	1.0	0.38	9.9	3.8
yes	10	0.63	0.21	0.64	0.21	6.5	1.9
yes	20	0.39	0.17	0.39	0.17	3.9	1.3
no	2	0	0.19	0	0.16	0	0.63
no	10	0	0.13	0	0.12	0	0.62
no	20	0	0.12	0	0.12	0	0.56

C. Integrator Response to a Transmitted Signal

Computational results of the statistical parameters of the correlator output are presented in Table I, derived from computer simulations and, where available, compared with analytical results. In the simulated system, $N_f = 10$ and $T_f = 10$ ns, implying a data rate of 10 Mbit/s. Random time-hopping codes were used. Again, good agreement is observed between both results.

It is evident that the proposed straight-forward multiuser-DTR receiver can work in situations with severe inter-frame-interference. An enhanced MU-receiver may exploit knownledge of the interference among pulses (*cf.* [3]).

VII. Conclusions

In this paper, the effect of (heavy) multipath interference (inter-frame interference (IFI)) on (differential) transmitted reference UWB systems is investigated statistically. The results can be expressed in terms of channel parameters like the RMS delay spread, average received power, and Ricean K-factor. It is observed that the results are largely independent of the exact distribution functions of the ray amplitudes or ray arrival times. An impact of the received prototype pulse is evident. The results can be used in the performance evaluation and optimization of TR-UWB systems.

Topics for further work are, next to the issues indicated throughout the paper, an evaluation of IFI for more detailed channel models and/or actual channel measurements, and the study of the impact of channel effects that have been neglected in the current paper.

References

[1] R. Hoctor and H. Tomlinson, 'Delay-hopped transmitted-reference RF communications," in *IEEE Conference on Ultra Wideband Systems and Technologies*, 2002, pp. 265–270.

[2] Y.-L. Chao and R. A. Scholtz, 'Optimal and suboptimal receivers for ultra-wideband transmitted reference systems," in *IEEE Global Telecommunications Conference, GLOBECOM*, San Francisco, CA, Dec. 2003.

[3] A. Trindade, Q. Dang, and A.-J. van der Veen, 'Signal processing model for a transmit-reference UWB wireless communication system," in *IEEE Conference on Ultra Wideband Systems and Technologies*, 2003.

[4] J. Choi and W. Stark, 'Performance of ultra-wideband communications with suboptimal receivers in multipath channels," *IEEE Journal on Selected Areas in Communications*, vol. 20, no. 9, pp. 1754–1766, Dec. 2002.

[5] K. Witrisal, 'OFDM air-interface design for wireless multimedia communications," Ph.D. dissertation, Delft University of Technology, Delft, The Netherlands, Apr. 2002. [Online]. Available: http://spsc.inw.tugraz.at/klaus/Thesis.pdf